Progress In Electromagnetics Research M, Vol. 99, 1–12, 2021

Self-Calibration Algorithm with Gain-Phase Errors Array for Robust DOA Estimation

Zhenyu Wei*, Wei Wang*, Fuwang Dong, and Ping Liu

Abstract—The performance of direction-of-arrival (DOA) estimation algorithms degrades when a partly calibrated array is adopted due to the existing unknown gain-phase uncertainties. In addition, the spatial discretized searching grid also limits the performance improvement and effectiveness of subspace-based DOA estimation algorithms, especially when the true angles do not lie on the grid points which is referred to the off-grid problem alike. In this paper, a self-calibration DOA estimation algorithm is proposed which solves the array calibration and off-grid problems simultaneously. Firstly, the signal model for a partly calibrated array with gain-phase uncertainties is established. To suppress the off-grid errors, an optimization problem for joint parameters estimation is constructed by substituting the approximation of the steering vector into a newly constructed objective function. The alternative minimization (AM) algorithm is employed to calculate the joint DOA and gain-phase uncertainty estimations. Within each iteration step of the optimization problem, a closed-form solution is derived that guarantees the convergence of the proposed algorithm. Furthermore, the Cramér-Rao bound (CRB) for the partly calibrated arrays with unknown gain-phase uncertainties is also derived and analyzed in the paper. Simulation results demonstrate the effectiveness of the proposed algorithm.

1. INTRODUCTION

Array signal processing, including direction-of-arrival (DOA) [1, 2], beamforming [3, 4], and imaging [5], has received intense attention in the past decades. DOA estimation is an essential technique, so is widely used in applications of radar, sonar, wireless communications, and radio imaging. In recent years, various DOA estimation algorithms have been proposed, including the Capon algorithm, maximum likelihood (ML) algorithms, multiple signal classification (MUSIC) algorithm, and the estimation of parameters via the rotational invariance technique (ESPRIT). In addition, advanced with the recently developed sparse signal reconstruction (SSR) scheme, several DOA algorithms have been proposed by exploiting the spatial sparse property [6–8].

Unfortunately, antenna arrays usually suffer from imperfections including the gain-phase uncertainties, mutual couplings, and antenna position errors in practice [9–11]. Thus, DOA estimation performance, especially for the antenna sensitive algorithms, will be significantly degraded with the array imperfections. To address this practical problem, the partly calibrated array model was established in [11], where unknown array errors are estimated jointly with the DOAs using the same data. In addition, several algorithms [12–16] have been developed to suppress the effects of antenna imperfections and improve the estimation performance by taking into account the array model errors. The algorithm in [12] constructed the MUSIC spectrum search function by considering the gain-phase uncertainties: two subsets of parameters are then estimated through a two-step iterative operation. In [13], a new cost function was constructed by minimizing the consistency between the manifold matrix and signal

Received 7 September 2020, Accepted 7 November 2020, Scheduled 22 November 2020

* Corresponding author: Zhenyu Wei (g-weizhenyu@hrbeu.edu.cn), Wei Wang (wangwei407@hrbeu.edu.cn).

The authors are with the College of Intelligent System Science and Engineering, Harbin Engineering University, Harbin, Heilongjiang 150001, China.

subspace. Unfortunately, the algorithms proposed in [12, 13] are extremely computationally complex and failed to guarantee convergence. The DOA estimation algorithm for partly calibrated array developed in [14] overcame the suboptimal performance and worked even with large phase errors. By considering the existence of gain-phase uncertainties in the array rotational invariance, an ESPRIT-like algorithm was developed in [15] which simultaneously provided closed-form expressions of the DOA and gain-phase uncertainties. The authors in [16] proposed a self-calibration approach with perturbed arrays by using redundancies in the virtual array. Recently, similar works considering gain-phase errors and self-calibration are also be done in [17, 18] under different scenarios.

In a more challenging scenario, the spectrum searching based DOA estimation algorithms, including the MUSIC and Capon algorithms, also suffer from off-grid problem as faced in the SSR-based DOA estimation algorithms [19–21]. It is because the spectrum searching based DOA estimation algorithms require a pre-specified discretized spatial grid with a finite number of elements, and they are derived under the assumption that the true DOAs fall on the grid points. However, the above assumption may not be always guaranteed in practice which will trigger off-grid errors. In order to address this problem, a Taylor expansion model was established to approximate the real steering vector [19]. Moreover, to further suppress the off-grid errors, a gridless convex optimization problem was formulated in [20] to achieve accurate DOA estimation. A dense grid or grid refinement was proposed in [21]. Unfortunately, it will straightforwardly lead to heavy computational complexity which makes it difficult to implement in practical applications. Thus, necessary operation should be taken to address this problem.

In this paper, a self-calibration algorithm with gain-phase error array is proposed for robust DOA estimation which addresses the array calibration and off-grid problem simultaneously. By considering the gain-phase uncertainties, the signal model for the partly calibrated array is first established. Utilizing the orthogonality between the signal and noise subspaces, a novel objective function is constructed. To suppress the effect of off-grid error, the objective function is modified by adopting the approximation of the steering vector. Then, the alternating minimization (AM) algorithm is employed to iteratively estimate the three subsets of unknown parameters, i.e., DOAs, off-grid errors, and gain-phase uncertainties. Thus, the array is self-calibrated with the estimated gain-phase uncertainties which improves the performance of the DOA estimation. In order to theoretically analyze the performance, the Cramér-Rao bound (CRB) is derived which considers the interaction of DOA as well as gain-phase errors. The superior performance of the proposed algorithm is demonstrated through the simulation results.

The main contributions of this paper are summarized as follows: 1) A novel objective function is constructed for joint estimation of DOA and gain-phase uncertainties. 2) A closed-form solution of the off-grid errors is derived which guarantees the convergence of the proposed algorithm, and the AM algorithm is employed as an efficient solver.

The rest of paper is organized as follows. In Section 2, the signal model of the partly calibrated array used in this paper is introduced. The proposed novel off-grid calibration algorithm is given in Section 3. Then, the derivation of the CRBs and simulation results are provided in Section 4. The conclusions are summarized in Section 5.

Notations: Upper-case (lower-case) bold characters are used to denote matrices (vectors). $\mathbf{I}_M$ is the $M \times M$ identity matrix and $\mathbf{1}_M$ is an $M \times 1$ all-one vector. $\mathbb{C}^{M\times N}$ ($\mathbb{C}^M$) denotes the $M \times N$ ($M \times 1$) matrix (vector) in the complex value domain. trace$\{\mathbf{A}\}$ is the trace of matrix $\mathbf{A}$. $\|\mathbf{x}\|_1$ and $\|\mathbf{x}\|_2$ stand for the ℓ_1-norm and ℓ_2-norm of vector $\mathbf{x}$, respectively. $(\cdot)^T$, $(\cdot)^*$ and $(\cdot)^H$ denote the transpose, conjugate and Hermitian operations of a matrix or a vector, respectively. E$[\cdot]$ is the statistic expectation operator. diag$\{\mathbf{x}\}$ stands for a diagonal matrix that uses the elements of $\mathbf{x}$ as its diagonal elements. $\Re\{\cdot\}$ is the real part of a matrix or vector. $\circ$ denotes the Schur-Hadamard product.

2. PARTLY CALIBRATED ARRAY SIGNAL MODEL

Consider a uniform linear array (ULA) consisting of M omni-directional antennas with inter-sensor spacing $d = \lambda/2$, where λ stands for the wavelength of received signal. We assume that there are K uncorrelated far-field sources impinging on the array from distinct directions $\boldsymbol{\theta} = [\theta_1, \ldots, \theta_K]^T$, where $\theta_k \in [-\frac{\pi}{2}, \frac{\pi}{2}]$. Thus, the complex-valued baseband received signal vector at time index t can be expressed

as

$$\mathbf{x}(t) = \sum_{k=1}^{K} \mathbf{a}(\theta_k) s_k(t) + \mathbf{n}(t) = \mathbf{A}\mathbf{s}(t) + \mathbf{n}(t), \tag{1}$$

where $\mathbf{a}(\theta_k) = [1, e^{-\jmath 2\pi d/\lambda \sin(\theta_k)}, \ldots, e^{-\jmath 2\pi (M-1) d/\lambda \sin(\theta_k)}]^T \in \mathbb{C}^M$ is the steering vector corresponding to the kth source. $\mathbf{A} = [\mathbf{a}(\theta_1), \ldots, \mathbf{a}(\theta_K)] \in \mathbb{C}^{M\times K}$ is the manifold matrix of sensors array, and $\mathbf{s}(t) = [s_1(t), \ldots, s_K(t)]^T \in \mathbb{C}^K$ is the source signal vector. Herein, $\mathbf{n}(t)$ denotes the noise term which obeys the Gaussian distribution with zero mean and variance matrix $\sigma_n^2 \mathbf{I}_M$, and we assume that the source signals and the noise term are uncorrelated.

The signal model in Eq. (1) is established under the assumption that the array is fully calibrated. In practice, some antennas of the array may not be fully calibrated and there exist gain-phase uncertainties in the array response. This kind of array is referred as partly calibrated array. Without loss of generality, we assume that the first M_c antennas are well calibrated, whereas the last $M - M_c$ antennas are uncalibrated with unknown gain and phase uncertainties. For analysis convenience, we further assume that the gain and phase uncertainties are time-invariant and angle-independent. In this case, the received signal vector $\bar{\mathbf{x}}(t)$ of the partly calibrated array can be rewritten as

$$\begin{aligned} \bar{\mathbf{x}}(t) &= \Gamma(\boldsymbol{\gamma})\mathbf{A}\mathbf{s}(t) + \mathbf{n}(t) \\ &= \bar{\mathbf{A}}\mathbf{s}(t) + \mathbf{n}(t), \end{aligned} \tag{2}$$

where $\Gamma(\boldsymbol{\gamma}) = \mathrm{diag}(\boldsymbol{\gamma})$ with the gain-phase uncertainties vector $\boldsymbol{\gamma} = [\mathbf{1}_{M_c}^T, \rho_1 e^{\jmath\varphi_1}, \ldots, \rho_{M-M_c} e^{\jmath\varphi_{M-M_c}}]^T$. ρ_m and φ_m are the gain and phase error of the mth antenna, respectively, $m \in \{1, \ldots, M - M_c\}$. $\bar{\mathbf{A}} = \Gamma(\boldsymbol{\gamma})\mathbf{A}(\boldsymbol{\theta})$ is the manifold matrix of the partly calibrated ULA. To the end, the corresponding sampling covariance matrix is evaluated using T collected samples, expressed as,

$$\hat{\bar{\mathbf{R}}} = \frac{1}{T} \sum_{t=1}^{T} \bar{\mathbf{x}}(t) \bar{\mathbf{x}}^H(t). \tag{3}$$

The eigendecomposition of $\hat{\bar{\mathbf{R}}}$ can be denoted as

$$\hat{\bar{\mathbf{R}}} = \hat{\bar{\mathbf{E}}}_s \hat{\bar{\mathbf{\Lambda}}}_s \hat{\bar{\mathbf{E}}}_s^H + \hat{\bar{\mathbf{E}}}_n \hat{\bar{\mathbf{\Lambda}}}_n \hat{\bar{\mathbf{E}}}_n^H. \tag{4}$$

where $\mathbf{\Lambda}_s$ and $\mathbf{\Lambda}_n$ are diagonal matrices consisting of K largest eigenvalues and $M - K$ smallest eigenvalues, respectively. The terms $\bar{\mathbf{E}}_s \in \mathbb{C}^{M\times K}$ and $\bar{\mathbf{E}}_n \in \mathbb{C}^{M\times M-K}$ are the corresponding eigenvectors, which spans the signal subspace and the noise subspace, respectively. Thus, the DOAs can be achieved by finding the K peaks of the following spectrum function

$$P_{\mathrm{MUSIC}} = \frac{1}{\bar{\mathbf{a}}^H(\phi_l) \hat{\bar{\mathbf{E}}}_n \hat{\bar{\mathbf{E}}}_n^H \bar{\mathbf{a}}(\phi_l)}, \tag{5}$$

with $\bar{\mathbf{a}}(\phi_l) = \Gamma(\boldsymbol{\gamma})\mathbf{a}(\phi_l)$, where ϕ_l is the lth element of $\mathbf{\Theta}$, and $\mathbf{\Theta} = [\phi_1, \ldots, \phi_L]$ is the L-element uniformly discretized spatial grid with step size τ in the range of $[-\pi/2, \pi/2]$.

3. THE PROPOSED ALGORITHM

By taking into account the partly calibrated array model, the joint DOA and gain-phase uncertainties estimation can be achieved by solving the following optimization problem

$$\begin{aligned} (\hat{\boldsymbol{\theta}}, \hat{\boldsymbol{\gamma}}) = \arg \min_{\phi_l \in \mathbf{\Theta}, \boldsymbol{\gamma}} \bar{\mathbf{a}}^H(\phi_l) \hat{\bar{\mathbf{E}}}_n \hat{\bar{\mathbf{E}}}_n^H \bar{\mathbf{a}}(\phi_l) = \left\| \bar{\mathbf{a}}^H(\phi_l) \hat{\bar{\mathbf{E}}}_n \right\|_2^2 \\ \text{s.t. } \gamma_m = 1, \quad m = 1, 2, \ldots, M_c, \end{aligned} \tag{6}$$

where γ_m is the mth element of $\boldsymbol{\gamma}$, and the constraint function is achieved based on the assumption that the first M_c sensors are fully calibrated.

According to the MUSIC spectrum function in Eq. (5), the performance of the conventional MUSIC algorithm relies on the division of the discretized spatial grid and assumes that the DOAs locate on the discretized grid points. In practice, this on-grid assumption is not always guaranteed which is referred

as off-grid problem. Under the off-grid scenario, the true DOAs do not lie on the grid points, i.e., $\theta_k \notin \mathbf{\Theta}$, $k = 1, \ldots, K$. In this case, the conventional MUSIC algorithm will never achieve accurate DOA estimation and suffers from degraded estimate performance. To suppress the effect of the off-grid problem, a dense grid or the grid refinement operation is necessary to reduce the off-grid error. However, the dense grid or grid refinement worsens the computational complexity. In addition, the true DOAs are selected from the continuous space domain, so the grid refinement operation cannot solve the off-grid problem for the MUSIC algorithm fundamentally. To suppress the off-grid errors, the approximation of the steering vector $\mathbf{a}(\theta_k)$, by utilizing the first order Taylor series expansion, can be expressed as,

$$\mathbf{a}(\theta_k) \approx \mathbf{a}(\phi_{l_k}, \beta_k) = \mathbf{a}(\phi_{l_k}) + \mathbf{b}(\phi_{l_k})\beta_k, \tag{7}$$

where ϕ_{l_k} is the grid point closest to the true DOA θ_k, and β_k is the corresponding off-grid error which is defined as $\beta_k = \theta_k - \phi_{l_k}$. Moreover, β_k is in the range of $[-\tau/2, \tau/2]$ with τ being the searching step. The vector $\mathbf{b}(\phi_{l_k})$ is the derivative of $\mathbf{a}(\phi_{l_k})$, i.e., $\mathbf{b}(\phi_{l_k}) = \partial\mathbf{a}(\phi_{l_k})/\partial\phi_{l_k}$. Compared with $\mathbf{a}(\phi_{l_k})$, the model error of $\mathbf{a}(\phi_{l_k}, \beta_k)$ is smaller, and the off-grid error can be consequently suppressed.

By substituting the steering vector approximation of $\mathbf{a}(\theta_k)$ into the optimization problem in (6), the optimization problem can be further expressed as

$$\begin{aligned}(\hat{\boldsymbol{\phi}}, \hat{\boldsymbol{\beta}}, \hat{\boldsymbol{\gamma}}) = \arg \min_{\phi_l \in \mathbf{\Theta}, \gamma} \ & \left\| [\Gamma(\boldsymbol{\gamma})\mathbf{a}(\phi_l, \beta_l)]^H \hat{\bar{\mathbf{E}}}_n \right\|_2^2 \\ \text{s.t. } & \mathbf{W}\boldsymbol{\gamma} = \mathbf{1}_{M_c},\end{aligned} \tag{8}$$

where $\hat{\boldsymbol{\phi}} = [\hat{\phi}_{l_1}, \ldots, \hat{\phi}_{l_K}]^T$ and $\hat{\boldsymbol{\beta}} = [\hat{\beta}_1, \ldots, \hat{\beta}_K]^T$. $\hat{\phi}_{l_k}$ is the coarse DOA estimation of the kth source by finding the kth peak with the discretized grid $\mathbf{\Theta}$, and $\hat{\beta}_k$ is the corresponding off-grid error estimation. Thus, accurate DOA estimation can be calculated as

$$\hat{\boldsymbol{\theta}} = \hat{\boldsymbol{\phi}} + \hat{\boldsymbol{\beta}}. \tag{9}$$

In addition, $\hat{\boldsymbol{\gamma}}$ is the estimated gain-phase uncertainties vector and $\mathbf{W} = [\mathbf{I}_{M_c}, \mathbf{0}_{M_c \times (M-M_c)}]$, and $\mathbf{0}_{M_c \times (M-M_c)}$ represents the $M_c \times (M - M_c)$ matrix where all entries are zero.

According to the uncorrelated property, the off-grid errors for different sources can be estimated separately. In this case, the optimization problem in Eq. (8) is converted into K sub-problems

$$\begin{aligned}\min_{\gamma, \beta_k} f(\boldsymbol{\gamma}, \beta_k) = & \boldsymbol{\gamma}^H \mathbf{P}_{1_k} \boldsymbol{\gamma} + 2\beta_k \Re\{\boldsymbol{\gamma}^H \mathbf{P}_{2_k} \boldsymbol{\gamma}\} + {\beta_k}^2 \boldsymbol{\gamma}^H \mathbf{P}_{3_k} \boldsymbol{\gamma} \\ \text{s.t. } & \mathbf{W}\boldsymbol{\gamma} = \mathbf{1}_{M_c},\end{aligned} \tag{10}$$

where

$$\begin{aligned}\mathbf{P}_{1_k} &= (\hat{\bar{\mathbf{E}}}_n \hat{\bar{\mathbf{E}}}_n^H) \circ (\mathbf{a}(\phi_{l_k})\mathbf{a}^H(\phi_{l_k}))^T \\ \mathbf{P}_{2_k} &= (\hat{\bar{\mathbf{E}}}_n \hat{\bar{\mathbf{E}}}_n^H) \circ (\mathbf{a}(\phi_{l_k})\mathbf{b}^H(\phi_{l_k}))^T \\ \mathbf{P}_{3_k} &= (\hat{\bar{\mathbf{E}}}_n \hat{\bar{\mathbf{E}}}_n^H) \circ (\mathbf{b}(\phi_{l_k})\mathbf{b}^H(\phi_{l_k}))^T,\end{aligned} \tag{11}$$

$k = 1, 2, \ldots, K$. The detailed derivations of Eq. (10) can be found in Appendix A. Note that the coarse DOA estimation $\hat{\phi}_{l_k}$ in Eq. (11) is obtained by finding the kth peak of MUSIC spectrum, and it has large estimation error due to the existence of the gain-phase uncertainties and off-grid error. Thus, to further improve the DOA estimation performance, the gain-phase uncertainties and off-grid errors should be further estimated.

It is well known that the AM algorithm [22] is an effective tool to solve the optimization problem involved several different subsets of variables, which is employed to solve the optimization problem in Eq. (10) in this paper. Without loss of generality, the off-grid errors are estimated first by fixing the gain-phase uncertainties. Hence, the objective function in Eq. (10) can be converted to a quadratic function with respect to β_k, i.e.,

$$f(\beta_k) = (\boldsymbol{\gamma}^H \mathbf{P}_{3_k} \boldsymbol{\gamma}){\beta_k}^2 + (2\Re\{\boldsymbol{\gamma}^H \mathbf{P}_{2_k} \boldsymbol{\gamma}\})\beta_k + \boldsymbol{\gamma}^H \mathbf{P}_{1_k} \boldsymbol{\gamma}. \tag{12}$$

Obviously, the optimal solution of $\hat{\beta}_k$ can be expressed in closed-form as

$$\hat{\beta}_k = -\frac{\Re\{\boldsymbol{\gamma}^H \mathbf{P}_{2_k} \boldsymbol{\gamma}\}}{\boldsymbol{\gamma}^H \mathbf{P}_{3_k} \boldsymbol{\gamma}}. \tag{13}$$

To further estimate the gain-phase uncertainties, β_k is fixed. Note that $\Re\{\boldsymbol{\gamma}^H\mathbf{P}_{2_k}\boldsymbol{\gamma}\} = (\boldsymbol{\gamma}^H\mathbf{P}_{2_k}\boldsymbol{\gamma} + \boldsymbol{\gamma}^H\mathbf{P}_{2_k}^H\boldsymbol{\gamma})/2$, and the optimization problem in Eq. (10) can be rewritten as

$$\begin{aligned} &\min_{\boldsymbol{\gamma}} \boldsymbol{\gamma}^H\mathbf{Q}_k\boldsymbol{\gamma} \\ &s.t. \mathbf{W}\boldsymbol{\gamma} = \mathbf{1}_{M_c}, \end{aligned} \tag{14}$$

with $\mathbf{Q}_k = \mathbf{P}_{1_k} + \beta_k(\mathbf{P}_{2_k} + \mathbf{P}_{2_k}^H) + \beta_k^2\mathbf{P}_{3_k}$. The optimization problem in Eq. (14) can be solved effectively using the Lagrange multiplier method, and the corresponding Lagrangian function is formulated as follows

$$L(\boldsymbol{\gamma}, \boldsymbol{u}) = \boldsymbol{\gamma}^H\mathbf{Q}_k\boldsymbol{\gamma} + \boldsymbol{u}^H(\mathbf{W}^H\boldsymbol{\gamma} - \mathbf{1}_{M_c}), \tag{15}$$

where $\boldsymbol{u}$ is the Lagrange multiplier vector. Let the partial derivative of $L(\boldsymbol{\gamma}, \boldsymbol{u})$ with respect to $\boldsymbol{\gamma}$ be zero, and the first-order necessary condition for optimal solution can be expressed as $\mathbf{Q}_k^T\boldsymbol{\gamma}^* + \mathbf{W}^*\boldsymbol{u}^* = \mathbf{0}$. To the end, we have,

$$\boldsymbol{\gamma} = -\mathbf{Q}_k^{-H}\mathbf{W}\boldsymbol{u}. \tag{16}$$

By substituting Eq. (16) into the constraint function of Eq. (14), the Lagrange multiplier $\boldsymbol{u}$ can be determined. Thus, the optimal solution of Eq. (14) can be expressed by

$$\hat{\boldsymbol{\gamma}}_k = \mathbf{Q}_k^{-H}\mathbf{W}(\mathbf{W}^H\mathbf{Q}_k^{-H}\mathbf{W})^{-1}\mathbf{1}_{M_c}. \tag{17}$$

To the end, β_k and $\boldsymbol{\gamma}_k$ are alternatively iterated until the convergence conditions are achieved. Once the iterative process is converged, the joint estimations of DOA and gain-phase uncertainties can be obtained. Note that the gain-phase uncertainties $\boldsymbol{\gamma}_k$ can be calculated using K different DOA estimations separately, and the estimation of $\hat{\boldsymbol{\gamma}}$ is achieved by averaging the K estimations, i.e.,

$$\hat{\boldsymbol{\gamma}} = \sum_{k=1}^{K} \boldsymbol{\gamma}_k/K. \tag{18}$$

In addition, the gain and phase estimations can be respectively obtained as follows

$$\begin{cases} \hat{\boldsymbol{\rho}}_l = |\hat{\boldsymbol{\gamma}}(M_c + l)| \\ \hat{\boldsymbol{\varphi}}_l = \angle(\hat{\boldsymbol{\gamma}}(M_c + l)) \end{cases}, \quad l = 1, \ldots, M - M_c. \tag{19}$$

where $\hat{\boldsymbol{\rho}} = [\hat{\rho}_1, \ldots, \hat{\rho}_{M-M_c}]^T$ and $\hat{\boldsymbol{\varphi}} = [\hat{\varphi}_1, \ldots, \hat{\varphi}_{M-M_c}]^T$. For simplification, the main steps of the proposed off-grid calibration algorithm which is referred as OGCA are summarized in Algorithm 1.

Algorithm 1. Off-Grid Calibration Algorithm

Initialization the gain-phase uncertainties matrix $\Gamma(\boldsymbol{\gamma}) = \mathbf{I}_M$, $i = 0$, $k = 1$;
Step 1 Obtain coarse DOA estimation $\hat{\boldsymbol{\phi}}$ by finding the K peaks of the conventional MUSIC spectrum;
Step 2 Let $\Gamma(\boldsymbol{\gamma}_k^{(i)}) = \mathbf{I}_M$;
Step 3 Fix $\boldsymbol{\gamma}_k^{(i)}$, optimize $\beta_k^{(i)}$ according to (13);
Step 4 Fix $\beta_k^{(i)}$, update $\boldsymbol{\gamma}_k^{(i+1)}$ with (17);
If $||\beta_k^{(i)} - \beta_k^{(i-1)}||_2 \leq \epsilon_1$ and $||\boldsymbol{\gamma}_k^{(i)} - \boldsymbol{\gamma}_k^{(i)-1}||_2 \leq \epsilon_2$ (ϵ_1 and ϵ_2 are thresholds), the iteration is terminated. Otherwise, let $i = i + 1$, and repeat **Step 3** and **4**.
Step 5 Let $k = k + 1$, $i = 0$.
Repeat **Step 2** to **Step 5** until all K off-grid errors $\hat{\boldsymbol{\beta}}$ are obtained.
Step 6 Calculate the accurate DOA estimation and the gain-phase uncertainties estimation through (9) and (18), respectively.

Remark: From Eq. (16), it is clear that the matrix $\mathbf{Q}_k$ should be a nonsingular or full-rank matrix. Otherwise, the estimation performance of $\boldsymbol{\gamma}$ will be heavily degraded. In order to avoid the singular case of matrix $\mathbf{Q}_k$, the diagonal loading method [23] can be adopted, that is, $\mathbf{Q}_{DL_k} = \mathbf{Q}_k + \delta\mathbf{I}$ where δ is the small diagonal loading factor. Indeed, the matrix $\mathbf{Q}_k$ is nonsingular within the extensive experience that we have made. Thus, the diagonal loading method is not necessary in general.

Convergence analysis: Actually, the objective function $f(\boldsymbol{\gamma}, \beta_k)$ in Eq. (10) is monotonically non-increasing in each iteration, i.e., $f(\hat{\boldsymbol{\gamma}}^{(i+1)}, \hat{\beta}_k^{(i+1)}) \leq f(\hat{\boldsymbol{\gamma}}^{(i)}, \hat{\beta}_k^{(i+1)}) \leq f(\hat{\boldsymbol{\gamma}}^{(i)}, \hat{\beta}_k^{(i)})$, where $\hat{\boldsymbol{\gamma}}^{(i)}$ and $\hat{\beta}_k^{(i)}$ denote the parameter estimations for the ith iteration. Furthermore, the objective function is non-negative. Therefore, the convergence of proposed iterative algorithm can be obviously guaranteed with these two properties [22]. In addition, compared with the similar iterative algorithm in [19, 22], the closed-form solution is obtained in each sub-optimization problem, which can significantly reduce the computational complexity.

Complexity analysis: Besides the eigendecomposition with $\mathcal{O}(M^3)$ complexity, the proposed algorithm contains two loops: the number of iterations in outer loop is equal to the number of sources K, and N_{in} denote the number of iterations in inner loop. In each iteration, the closed-form formulations (13) and (17) are computed with complexity $\mathcal{O}(M^2)$ and $\mathcal{O}(M^3)$, respectively. Specifically, the dimensions of $\mathbf{P}_{i_k}, (i = 1, 2, 3)$ and $\mathbf{Q}_k$ are $M \times M$, and the most expensive complexity is the inverse operation with $\mathcal{O}(M^3)$ flops in Eq. (17). Consequently, the whole computational complexity of proposed algorithm is given by $\mathcal{O}(KN_{in}M^3)$.

4. SIMULATION RESULTS AND DISCUSSION

In this section, the closed-form expressions for CRBs are derived which consider the effect of gains and phases uncertainties. Simulation results are then provided to evaluate the performance of proposed algorithm by comparing the conventional MUSIC algorithms and CRBs.

4.1. CRBs Analysis

In this subsection, the CRBs are derived under the assumption that the received signal vectors of the partly calibrated array follow the zero-mean and statistically independent Gaussian distribution. In addition, three unknown parameter vectors including the DOAs $\boldsymbol{\theta}$, gains $\boldsymbol{\rho}$, and phases $\boldsymbol{\phi}$ are denoted as $\boldsymbol{\theta} = [\theta_1, \ldots, \theta_K]^T$, $\boldsymbol{\rho} = [\rho_1, \ldots, \rho_{M-M_c}]^T$ and $\boldsymbol{\varphi} = [\varphi_1, \ldots, \varphi_{M-M_c}]^T$, respectively. Compared to the existing CRBs expression [15], the derived CRBs consider the interaction between different unknown parameters.

With T snapshots of received signal, the elements of FIM with respect to the unknown parameter vector $\boldsymbol{z} = [\boldsymbol{\theta}^T, \boldsymbol{\rho}^T, \boldsymbol{\varphi}^T]^T$ are given by [13]

$$\mathbf{F}_{ij} = T\text{trace}\left\{\mathbf{R}^{-1}\frac{\partial \mathbf{R}}{\partial \boldsymbol{z}_i}\mathbf{R}^{-1}\frac{\partial \mathbf{R}}{\partial \boldsymbol{z}_j}\right\}, \tag{20}$$

where $\mathbf{R}$ is the covariance matrix of signal vector $\mathbf{x}(t)$; $\boldsymbol{z}_i$ and $\boldsymbol{z}_j$ denote the ith and jth elements of $\boldsymbol{z}$, respectively. As it is known, the CRBs are equal to the corresponding diagonal elements of the inverse of the FIM, $\mathbf{F} \triangleq [\mathbf{F}_{ij}]$. Therefore, the next step is to calculate the block elements of FIM, i.e., $\mathbf{F}_{ij}$. The DOA-DOA block of the FIM is given by

$$\mathbf{F}_{\theta\theta} = 2\Re\left\{(\mathbf{R}_s\bar{\mathbf{A}}^H\mathbf{R}^{-1}\bar{\mathbf{A}}\mathbf{R}_s) \circ (\dot{\bar{\mathbf{A}}}^H\mathbf{R}^{-1}\dot{\bar{\mathbf{A}}})^T + (\mathbf{R}_s\bar{\mathbf{A}}^H\mathbf{R}^{-1}\dot{\bar{\mathbf{A}}}) \circ (\mathbf{R}_s\bar{\mathbf{A}}^H\mathbf{R}^{-1}\dot{\bar{\mathbf{A}}})^T\right\}, \tag{21}$$

where

$$\dot{\bar{\mathbf{A}}} = \sum_{k=1}^{K}\frac{\partial \bar{\mathbf{A}}}{\partial \theta_k} = \Gamma(\boldsymbol{\gamma})\sum_{k=1}^{K}\frac{\partial \mathbf{A}}{\partial \theta_k}. \tag{22}$$

The DOA-gain block is calculated as

$$\mathbf{F}_{\theta\rho} = 2\Re\left\{\left[(\mathbf{R}_s\bar{\mathbf{A}}^H\mathbf{R}^{-1}) \circ (\mathbf{C}\mathbf{A}\mathbf{R}_s\bar{\mathbf{A}}^H\mathbf{R}^{-1}\dot{\bar{\mathbf{A}}})^T + (\mathbf{R}_s\bar{\mathbf{A}}^H\mathbf{R}^{-1}\bar{\mathbf{A}}\mathbf{R}_s\mathbf{A}^H\mathbf{C}^H) \circ (\mathbf{R}^{-1}\dot{\bar{\mathbf{A}}})^T\right]\mathbf{H}^T\right\}, \tag{23}$$

where $\mathbf{C} = \text{diag}([\mathbf{1}_{M_c}^T, \boldsymbol{\varphi}^T])$ and $\mathbf{H}$ is an $(M - M_c) \times M$ selection matrix with the (i, j)th element

$$[\mathbf{H}]_{i,j} = \begin{cases} 1, \text{ if } j = i + M_c \\ 0, \text{ otherwise.} \end{cases} \tag{24}$$

The DOA-phase block is expressed as

$$\mathbf{F}_{\theta\phi} = 2\Re\left\{\jmath\left[(\mathbf{R}_s\bar{\mathbf{A}}^H\mathbf{R}^{-1})\circ(\bar{\mathbf{A}}\mathbf{R}_s\bar{\mathbf{A}}^H\mathbf{R}^{-1}\dot{\bar{\mathbf{A}}})^T-(\mathbf{R}_s\bar{\mathbf{A}}^H\mathbf{R}^{-1}\bar{\mathbf{A}}\mathbf{R}_s\bar{\mathbf{A}}^H)\circ(\mathbf{R}^{-1}\dot{\bar{\mathbf{A}}})^T\right]\mathbf{H}^T\right\}. \quad (25)$$

The gain-gain block is given as

$$\begin{aligned}\mathbf{F}_{\rho\rho} &= 2\Re\left\{\mathbf{H}[(\mathbf{C}\mathbf{A}\mathbf{R}_s\bar{\mathbf{A}}^H\mathbf{R}^{-1})\circ(\mathbf{C}\mathbf{A}\mathbf{R}_s\bar{\mathbf{A}}^H\mathbf{R}^{-1})^T\right.\\ &\quad\left.+(\mathbf{C}\mathbf{A}\mathbf{R}_s\bar{\mathbf{A}}^H\mathbf{R}^{-1}\bar{\mathbf{A}}\mathbf{R}_s\mathbf{A}^H\mathbf{C}^H)\circ(\mathbf{R}^{-1})^T]\mathbf{H}^T\right\}. \quad (26)\end{aligned}$$

The gain-phase block is given by

$$\mathbf{F}_{\rho\phi} = 2\Re\left\{\jmath\mathbf{H}[(\mathbf{C}\mathbf{A}\mathbf{R}_s\bar{\mathbf{A}}^H\mathbf{R}^{-1})\circ(\bar{\mathbf{A}}\mathbf{R}_s\bar{\mathbf{A}}^H\mathbf{R}^{-1})^T-(\mathbf{C}\mathbf{A}\mathbf{R}_s\bar{\mathbf{A}}^H\mathbf{R}^{-1}\bar{\mathbf{A}}\mathbf{R}_s\bar{\mathbf{A}}^H)\circ(\mathbf{R}^{-1})^T]\mathbf{H}^T\right\}. \quad (27)$$

At last, the phase-phase block can be expressed as

$$\mathbf{F}_{\phi\phi} = 2\Re\left\{\mathbf{H}[(\bar{\mathbf{A}}\mathbf{R}_s\bar{\mathbf{A}}^H\mathbf{R}^{-1}\bar{\mathbf{A}}\mathbf{R}_s\bar{\mathbf{A}}^H)\circ(\mathbf{R}^{-1})^T-(\bar{\mathbf{A}}\mathbf{R}_s\bar{\mathbf{A}}^H\mathbf{R}^{-1})\circ(\bar{\mathbf{A}}\mathbf{R}_s\bar{\mathbf{A}}^H\mathbf{R}^{-1})^T]\mathbf{H}^T\right\}. \quad (28)$$

4.2. Simulation Results and RMSE Analysis

Without loss of generality, a partly calibrated ULA with $M = 10$ antennas is considered in this subsection. In addition, we assume that there are three ($K = 3$) far-field uncorrelated narrow-band signals impinging on the array. In order to demonstrate the superior performance of the proposed algorithm, the true DOAs of the three sources come from different directions $-15.4423°$, $0.3846°$, and $25.5828°$, respectively. In the following simulations, the first five sensors are assumed to be calibrated i.e., $M_c = 5$, and the last five sensors are uncalibrated with unknown gain-phase uncertainties given by $0.8e^{\jmath\pi/5}$, $1.25e^{-\jmath\pi/3}$, $1.53e^{-\jmath\pi/5}$, $0.75e^{\jmath\pi/4}$, and $1.36e^{-\jmath\pi/10}$. The signal to noise ratio (SNR) used in this paper is defined as

$$\mathrm{SNR} = 10\log\left(\mathrm{E}[\|\mathbf{s}(t)\|_2^2]/\mathrm{E}[\|\mathbf{n}(t)\|_2^2]\right). \quad (29)$$

To evaluate the DOA estimation performance, the root mean square error (RMSE) used in this paper is defined as

$$\mathrm{RMSE}_\theta = \sqrt{\frac{1}{KP}\sum_{p=1}^{P}\sum_{k=1}^{K}\left(\hat{\theta}_{p,k}-\theta_k\right)^2}. \quad (30)$$

where $\hat{\theta}_{p,k}$ is the estimation of DOA θ_k within the pth Monte Carlo trial, and P is the total number of the Monte Carlo trials and $P = 1000$. All simulations in this paper are operated via Matlab 2014a on a laptop platform with Windows 10 operation system.

In order to examine the performance of the proposed algorithm, the RMSE curves versus SNR of different DOA estimation and calibration algorithms are provided in Fig. 1. OGSBI and SURE_IR algorithms refer to the off-grid sparse Bayesian inference [19] and super-resolution iterative reweighted [24], respectively. The yellow squared line is referred to simultaneous orthogonal matching pursuit with total least squares (SOMP_TLS) [25]. The CRB curve is calculated with joint DOA and gain-phase estimation. In this simulation, the discretized grid is in the range of $-90°$ to $90°$ with the step size $\tau = 1°$. Note that the OGSBI and SURE_IR algorithms can tackle the off-grid problem effectively; however, they cannot address the gain-phase uncertainties. On the other hand, the SOMP_TLS is robust to the uncertainties; yet the off-grid error will cause a degradation of DOA estimation heavily. From these simulation results, the proposed self-calibration algorithm shows superior performance to the other approaches in the case of partly calibrated ULAs, especially with high SNRs. It is because the proposed algorithm can address the off-grid problem and gain-phase errors simultaneously. The performance of the conventional MUSIC algorithm achieves a floor RMSE curve even with the increasing of SNR, and the reason is that the existence of the off-grid error constrains the performance improvement. Note that the proposed algorithm has a poor performance compared to MUSIC, OGSBI, and SURE_IR algorithms at the period of lower SNR. The reason for this phenomenon is that when SNR is low, there exist larger biases in coarse DOA estimation while the errors will be accumulated during the AM iteration process with the negative impact of array uncertainties.

In addition, Fig. 2 depicts the RMSE comparison of DOA estimations versus the number of snapshots. In this simulation, the SNR is set as 10 dB while the step size of the discretized grid is

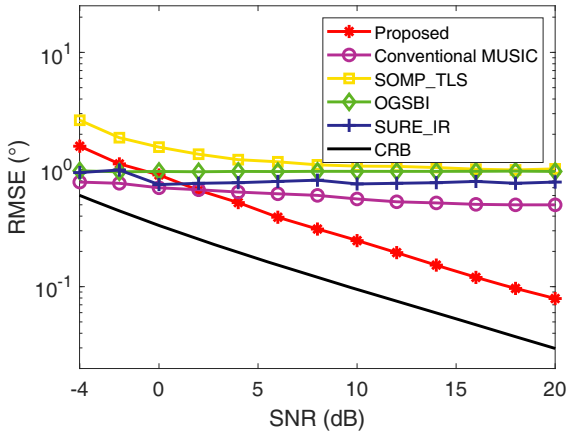

Figure 1. RMSE comparison versus SNR with different algorithms ($T = 500$).

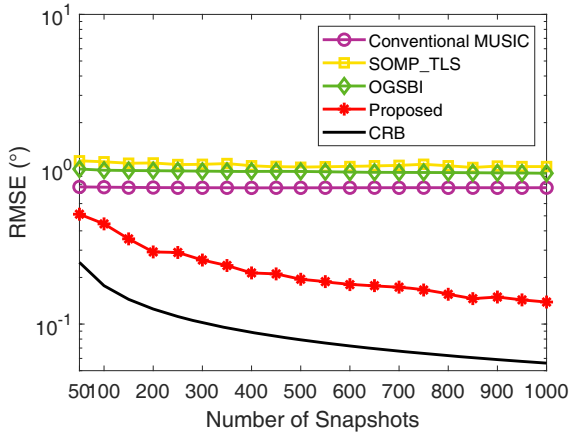

Figure 2. RMSE of DOA estimation versus the number of snapshots.

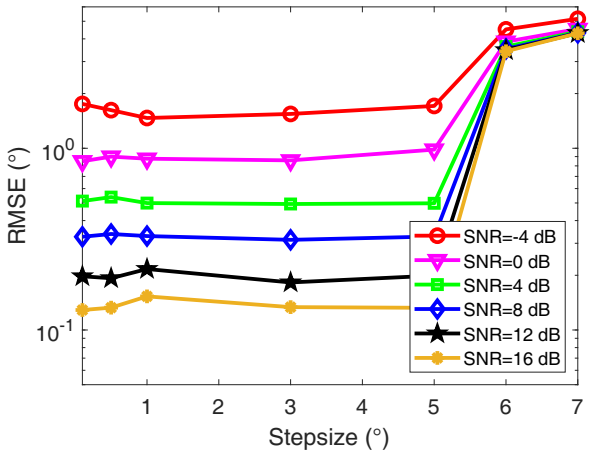

Figure 3. RMSE of DOA estimation versus step sizes with different SNR settings ($T = 500$).

$\tau = 1°$. The number of snapshots is varied from 50 to 1000. Since the proposed self-calibration algorithm can suppress the effect of off-grid error and gain-phase uncertainties at the same time, the proposed algorithm presents a better performance than the other algorithms whenever the number of snapshots changes.

As analyzed previously, the step size of the searching grid has a fundamental effect on the performance of conventional MUSIC. In order to examine the robustness of the proposed algorithm with different step sizes, the RMSE curves of DOA estimation are illustrated in Fig. 3. As shown in Fig. 3, the proposed algorithm still exhibits an acceptable result even when the step size $\tau = 5°$.

Figures 4 and 5 give the RMSE of gain-phase estimation versus SNR and the number of snapshots, respectively. In this two simulations, the step size is set as 3°. It shows that the proposed algorithm also has good performance on gain-phase estimation.

To further verify the convergence of the proposed algorithm, the values of the cost function in Eq. (10) versus iteration number at different SNRs are plotted in Fig. 6. It can be seen that the proposed DOA estimation algorithm always guarantees convergence within about 60 iterations.

In examining the resolution performance, the RMSE comparison of the proposed algorithm, MUSIC, SOMP_TLS, OGSBI, and SURE_IR algorithms is plotted in Fig. 7. In this simulation, two targets with different angle separations varying from 2.4° to 18° are considered. From Fig. 7, we can see that the RMSE values of all algorithms decrease with the increase of separation angle. Nevertheless,

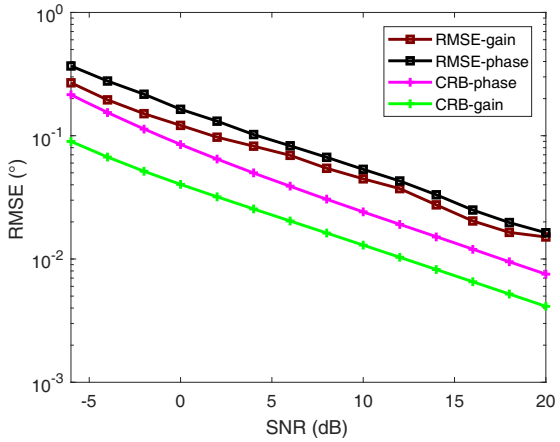

Figure 4. RMSE of phase-gain estimation versus SNR ($T = 500$).

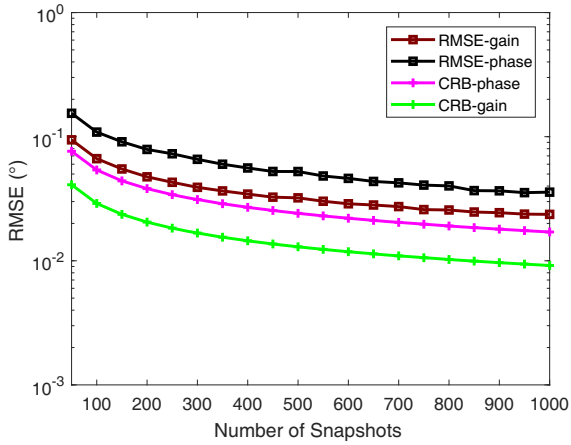

Figure 5. RMSE of phase-gain estimation versus snapshots (SNR $= 10$ dB).

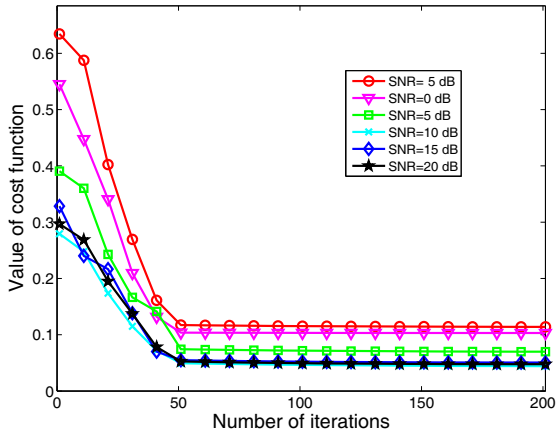

Figure 6. The value of the cost function versus iteration number with different SNR settings.

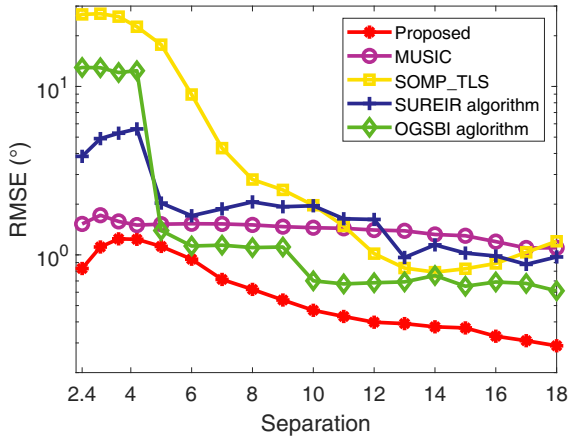

Figure 7. RMSE of DOA estimation versus angle separation ($T = 500$).

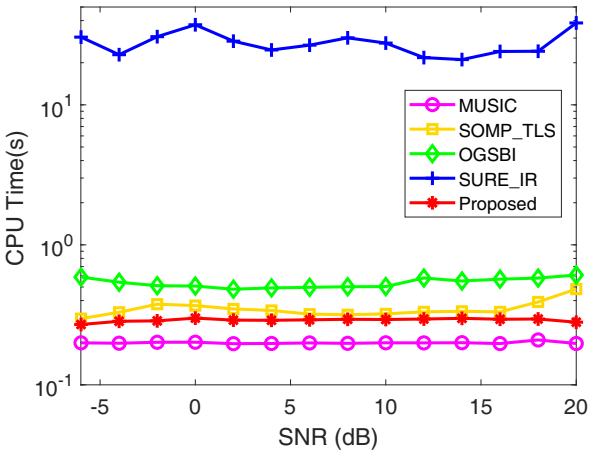

Figure 8. Averaged CPU running time versus SNR.

the proposed algorithm still achieves a better DOA estimation performance.

Finally, in order to verify the efficiency of the proposed self-calibration algorithm, the CPU running time of all test algorithms is compared in Fig. 8, where the curves are averaged in 50 Monte Carlo runs. It is obvious that the SURE_IR involves heave computational load, due to the severe non-convexity and pruning operation. On the other hand, the proposed method shows better efficient estimation performance with the benefit of the convergence, although the iterative process is adopted. For intuitive, the CPU running time is averaged among all different SNRs and listed in Table 1.

Table 1. Detailed CPU running time of respective algorithms averaged among all SNR settings.

Algorithms	MUSIC	SOMP_TLS	OGSBI	SURE_IR	Proposed
Running Time(s)	0.2029	0.3414	0.5406	27.1389	0.2905

5. CONCLUSION

This paper proposes a novel self-calibration algorithm that offers robust DOA estimation even with partly calibrated arrays. By utilizing the Taylor series expansion, the approximation of the steering vector is achieved which can suppress the off-grid error effectively. With the fact that the signal and noise subspaces are orthogonal to each other, a novel objective function is constructed which considers the gain-phase uncertainties. Thus, the joint estimation of DOA, gain-phase uncertainties, and off-grid errors can be iteratively estimated by solving the constructed objective function through the AM algorithm. At last, the CRB for partly calibrated array with unknown uncertainties is also derived which considers the interaction between different unknown parameters. Simulation results show the convergence performance and the effectiveness of the proposed algorithm.

ACKNOWLEDGMENT

The research is funded in part by the National Natural Science Foundation (61871143) of China, Ministry of industry and information technology [2019]331, Fundamental Research for the Central University (3072019CF0402), Heilongjiang Natural Science Foundation (LH2019F006) and Research and Development Project of Application Technology in Harbin (2017R-AQXJ095).

APPENDIX A. DERIVATION OF (10)

In this appendix, we provide the formula derivation of the optimization problem in Eq. (8). At first, the objective function in in Eq. (8) can be expanded according to the definition of ℓ_2-norm

$$\begin{aligned}
\left\|[\Gamma(\boldsymbol{\gamma})\mathbf{a}(\phi_l,\beta_l)]^H\hat{\tilde{\mathbf{E}}}_n\right\|_2^2 &= \left\|[\Gamma(\boldsymbol{\gamma})(\mathbf{a}(\phi_{l_k})+\beta_k\mathbf{b}(\phi_{l_k}))]^H\hat{\tilde{\mathbf{E}}}_n\right\|_2^2 \\
&= \mathbf{a}^H(\phi_{l_k})\Gamma^H(\boldsymbol{\gamma})\hat{\tilde{\mathbf{E}}}_n\hat{\tilde{\mathbf{E}}}_n^H\Gamma(\boldsymbol{\gamma})\mathbf{a}(\phi_{l_k}) + 2\beta_k\Re\{\mathbf{b}^H(\phi_{l_k})\Gamma^H(\boldsymbol{\gamma})\hat{\tilde{\mathbf{E}}}_n\hat{\tilde{\mathbf{E}}}_n^H\Gamma(\boldsymbol{\gamma})\mathbf{a}(\phi_{l_k})\} \\
&\quad + \beta_k^2\mathbf{b}^H(\phi_{l_k})\Gamma^H(\boldsymbol{\gamma})\hat{\tilde{\mathbf{E}}}_n\hat{\tilde{\mathbf{E}}}_n^H\Gamma(\boldsymbol{\gamma})\mathbf{b}(\phi_{l_k}) \\
&\overset{(a)}{=} \mathrm{trace}\{\mathbf{a}^H(\phi_{l_k})\Gamma^H(\boldsymbol{\gamma})\hat{\tilde{\mathbf{E}}}_n\hat{\tilde{\mathbf{E}}}_n^H\Gamma(\boldsymbol{\gamma})\mathbf{a}(\phi_{l_k})\} \\
&\quad + 2\beta_k\mathrm{trace}\{\Re\{\mathbf{b}^H(\phi_{l_k})\Gamma^H(\boldsymbol{\gamma})\hat{\tilde{\mathbf{E}}}_n\hat{\tilde{\mathbf{E}}}_n^H\Gamma(\boldsymbol{\gamma})\mathbf{a}(\phi_{l_k})\} \\
&\quad + \beta_k^2\mathrm{trace}\{\mathbf{b}^H(\phi_{l_k})\Gamma^H(\boldsymbol{\gamma})\hat{\tilde{\mathbf{E}}}_n\hat{\tilde{\mathbf{E}}}_n^H\Gamma(\boldsymbol{\gamma})\mathbf{b}(\phi_{l_k})\} \\
&\overset{(b)}{=} \mathrm{trace}\{\mathbf{a}(\phi_{l_k})\mathbf{a}^H(\phi_{l_k})\Gamma^H(\boldsymbol{\gamma})\hat{\tilde{\mathbf{E}}}_n\hat{\tilde{\mathbf{E}}}_n^H\Gamma(\boldsymbol{\gamma})\} \\
&\quad + 2\beta_k\mathrm{trace}\{\Re\{\mathbf{a}(\phi_{l_k})\mathbf{b}^H(\phi_{l_k})\Gamma^H(\boldsymbol{\gamma})\hat{\tilde{\mathbf{E}}}_n\hat{\tilde{\mathbf{E}}}_n^H\Gamma(\boldsymbol{\gamma})\} \\
&\quad + \beta_k^2\mathrm{trace}\{\mathbf{b}(\phi_{l_k})\mathbf{b}^H(\phi_{l_k})\Gamma^H(\boldsymbol{\gamma})\hat{\tilde{\mathbf{E}}}_n\hat{\tilde{\mathbf{E}}}_n^H\Gamma(\boldsymbol{\gamma})\}
\end{aligned}$$

$$\begin{aligned}
&\overset{(c)}{=} \boldsymbol{\gamma}^H(\hat{\tilde{\mathbf{E}}}_n\hat{\tilde{\mathbf{E}}}_n^H)\circ(\mathbf{a}(\phi_{l_k})\mathbf{a}^H(\phi_{l_k}))^T\boldsymbol{\gamma} + 2\beta_k\Re\{\boldsymbol{\gamma}^H(\hat{\tilde{\mathbf{E}}}_n\hat{\tilde{\mathbf{E}}}_n^H)\circ(\mathbf{a}(\phi_{l_k})\mathbf{b}^H(\phi_{l_k}))^T\boldsymbol{\gamma}\} \\
&\quad + \beta_k^2\boldsymbol{\gamma}^H(\hat{\tilde{\mathbf{E}}}_n\hat{\tilde{\mathbf{E}}}_n^H)\circ(\mathbf{b}(\phi_{l_k})\mathbf{b}^H(\phi_{l_k}))^T\boldsymbol{\gamma} \\
&= \boldsymbol{\gamma}^H\mathbf{P}_{1_k}\boldsymbol{\gamma} + 2\beta_k\Re\{\boldsymbol{\gamma}^H\mathbf{P}_{2_k}\boldsymbol{\gamma}\} + {\beta_k}^2\boldsymbol{\gamma}^H\mathbf{P}_{3_k}\boldsymbol{\gamma},
\end{aligned} \tag{A1}$$

where (a) and (b) follow the trace properties $a = \text{trace}(a)$ with a constant variable and $\text{trace}\{\mathbf{AB}\} = \text{trace}\{\mathbf{BA}\}$, respectively. In addition, (c) is derived based on the following identity

$$\text{trace}\left\{\mathbf{M}\text{diag}(\boldsymbol{u}^H)\mathbf{N}\text{diag}(\boldsymbol{u})\right\} = \boldsymbol{u}^H(\mathbf{N}\circ\mathbf{M}^T)\boldsymbol{u}, \tag{A2}$$

where $\mathbf{M}$ and $\mathbf{N}$ are $m \times m$ matrices and $\boldsymbol{u} = [u_1, u_2, \ldots, u_m]^T$. Thus, the derivation of Eq. (10) is finalized.

REFERENCES

1. Vorobyov, S., A. Gershman, and K. Wong, "Maximum likelihood direction-of-arrival estimation in unknown noise fields using sparse sensor arrays," *IEEE Trans. Signal Process.*, Vol. 53, No. 1, 34–43, Jan. 2005.
2. Wei, Z., W. Wang, B. Wang, P. Liu, and S. Gong, "Effective direction-of-arrival estimation algorithm by exploiting Fourier transform for sparse array," *IEICE Trans. Commun.*, Vol. E102-B, No. 11, 2159–2166, Nov. 2019.
3. Gu, Y. and A. Leshem, "Robust adaptive beamforming based on interference covariance matrix reconstruction and steering vector estimation," *IEEE Trans. Signal Process.*, Vol. 60, No. 7, 3881–3885, Jul. 2012.
4. Gu, Y., N. A. Goodman, S. Hong, and Y. Li, "Robust adaptive beamforming based on interference covariance matrix sparse reconstruction," *Signal Process.*, Vol. 96, No. PART B, 375–381, 2014.
5. Urco, J. M., L. Chau, J. Milla, A. M. Vierinen, P. J. and T. Weber, "Coherent MIMO to improve aperture synthesis radar imaging of field-aligned irregularities: First results at Jicamarca," *IEEE Trans. Geosci. Remote Sens.*, Vol. 56, No. 5, 2980–2990, May 2018.
6. Wei, Z., X. Li, B. Wang, W. Wang, and Q. Liu, "An efficient super-resolution DOA estimation based on grid learning," *Radioengineering*, Vol. 28, No. 4, 785–792, Dec. 2019.
7. Shi, Z., C. Zhou, Y. Gu, N. A. Goodman, and F. Qu, "Source estimation using coprime array: A sparse reconstruction perspective," *IEEE Sens. J.*, Vol. 17, No. 3, 755–765, Feb. 2017.
8. Wang, B., Y. D. Zhang, and W. Wang, "Robust group compressive sensing for DOA estimation with partially distorted observations," *EURASIP J. Adv, Signal Process.*, Vol. 2016, No. 1, Dec. 2016.
9. Yang, K., Z. Wu, and Q. H. Liu, "Robust adaptive beamforming against array calibration errors," *Progress In Electromagnetics Research*, Vol. 140, 341–351, 2013.
10. Baburs, G., D. Caratelli, and A. Mirmanov, "Phased array calibration by binary compressed sensing," *Progress In Electromagnetics Research M*, Vol. 73, 61–70, 2018.
11. Tuncer, E. and B. Freidlander, *Calibration in Array Processing: Classical and Modern Direction-of-arrival Estimation*, 1st Edition, Academic Press, 2009.
12. Weiss, A. and B. Friedlander, "Eigenstructure methods for direction finding with sensor gain and phase uncertainties," *Circuits Syst. Signal Process.*, Vol. 9, No. 3, 271–300, 1990.
13. Weiss, A. and B. Friedlander, "DOA and steering vector estimation using a partially calibrated array," *IEEE Trans. Aerosp. Electron. Syst.*, Vol. 32, No. 3, 1047–1057, Jul. 1996.
14. Liu, A., G. Liao, C. Zeng, Z. Yang, and Q. Xu, "An eigenstructure method for estimating DOA and sensor gain-phase errors," *IEEE Trans. Signal Process.*, Vol. 59, No. 12, 5944–5956, Dec. 2011.
15. Liao, B. and S. C. Chan, "Direction finding with partly calibrated uniform linear arrays," *IEEE Trans. Aerosp. Electron. Syst.*, Vol. 60, No. 2 PART 2, 922–929, Feb. 2012.
16. Koochakzadeh, A. and P. Pal, "Sparse source localization using perturbed arrays via bi-affine modeling," *Digital Signal Process.*, Vol. 61, No. 7, 15–25, Feb. 2017.

17. Wang, B., Y. D. Zhang, and W. Wang, "Robust DOA estimation in the presence of miscalibrated sensors," *IEEE Signal Process Lett.*, Vol. 24, No. 7, 1073–1077, Jul. 2017.
18. Liu, J., W. Zhou, D. Huang, and F. Juwono, "Covariance matrix based fast smoothed sparse DOA estimation with partly calibrated array," *AEU Int. J. Electron. Commun.*, Vol. 84, 8–12, Feb. 2018.
19. Yang, Z., L. Xie, and C. Zhou, "Off-grid direction of arrival estimation using sparse Bayesian inference," *IEEE Trans. Signal Process.*, Vol. 61, No. 1, 38–43, 2013.
20. Zhou, C., Y. Gu, J. Shi, and Y. D. Zhang, "Off-grid direction-of-arrival estimation using coprime array interpolation," *IEEE Signal Process Lett.*, Vol. 25, No. 11, 1710–1714, Nov. 2018.
21. Malioutov, D., M. Çetin, and A. S. Willsky, "A sparse signal reconstruction perspective for source localization with sensor arrays," *IEEE Trans. Signal Process.*, Vol. 53, No. 8, 3010–3022, 2005.
22. Yu, X., J. C. Shen, J. Zhang, and K. B. Letaief, "Alternating minimization algorithms for hybrid precoding in millimeter wave MIMO systems," *IEEE J. Sel. Top. Signal Process.*, Vol. 10, No. 3, 485–500, Apr. 2016.
23. Li, J. and P. Stoica, *Robust Adaptive Beamforming*, 1st Edition, Wiley-Interscience, 2006.
24. Fang, J., F. Wang, Y. Shen, H. Li, and R. S. Blum, "Super-resolution compressed sensing for line spectral estimation: An iterative reweighted approach," *IEEE Trans. Signal Process.*, Vol. 64, No. 18, 4649–4662, Sep. 2016.
25. Hu, B., X. Wu, X. Zhang, Q. Yang, and W. Deng, "DOA estimation based on compressed sensing with gain/phase uncertainties," *IET Radar Sonar Navig.*, Vol. 12, No. 11, 1346–1352, Sep. 2018.